

Characterization and Corrosion Properties of Thermally Sprayed Al-Co-Ce Alloys

Nicole Tailleart
Center for Electrochemical Science and Engineering
University of Virginia

Objective

To design a pulsed thermal spray (PTS) metal coating, for use in aerospace applications, with potent corrosion functions, including strong barrier, sacrificial anode, and inhibitor properties.

Motivation

Al-cladding suppresses exfoliation corrosion, pitting, and stress corrosion to a degree, but:

- lacks a sufficient potential driving force for extensive throwing power.
- lacks an active inhibitor.
- the benefits of cladding are lost during repair and cladding is not field replaceable.

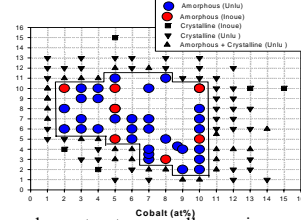
Coating Attributes

A “good” coating acts as barrier, sacrificial anode, and has inhibitor properties.

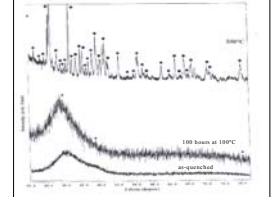
- **Barrier:** Defined by $E_{PIT}(Alloy) > E_{PIT}(AA\ 2024-T351)$, pore free, good coating-substrate adhesion, alloy composition (increased Co. conc.), an absence of intermetallic compounds, may desire amorphous structure to improve barrier.
- **Sacrificial Anode:** Defined by $E_{OCP}(Alloy) < E_{OCP}(AA\ 2024-T351)$, alloy composition (increased Ce conc., decreased Co conc.), minimum oxide on particles, may desire crystalline phases present.
- **Inhibitor:** Defined by release capability, alloy composition (increased Ce conc.), minimum oxide on particles, amorphous structure not required.

Alloy Development

Al-Co-Ce System Map¹

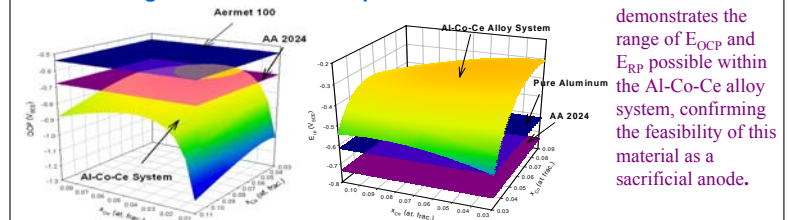


XRD Spectra of Al₈₇Co₇Ce₆ at% MSR²



- An amorphous structure usually requires cooling rates greater than $10^5\ K/s$.³
- XRD for the as-quenched melt-spun ribbon (MSR) and the crystalline microstructure of the isothermally high temperature heat-treated material at 100 °C for 100 hours and 550 °C shown above right (where ♦ indicates Al, ● indicates Al₃Co₂, and ■ Al₄Ce).
- The amorphous structure is stable even after significant heat treatment.

Model of E_{OCP} and E_{RP} for Al-Co-Ce Alloys Over Range of Co and Ce Compositions⁴



This model demonstrates the range of E_{OCP} and E_{RP} possible within the Al-Co-Ce alloy system, confirming the feasibility of this material as a sacrificial anode.

Coating Metallurgy

EDS Spectra for Feedstock Powder and PTS Coatings

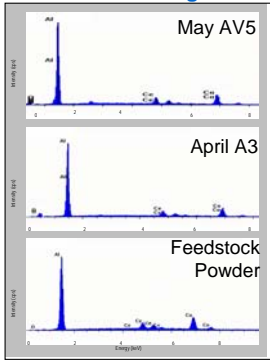
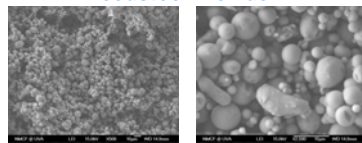


Table of Compositions: Expected vs. Actual

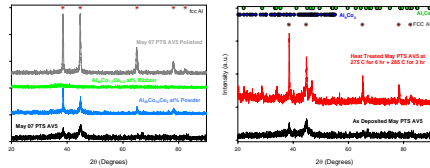
	Nominal Composition (at%)	Actual Composition (at%)
Powder	Al88-Co10-Ce2	Al81.6-Co13.7-Ce4.7
May PTS AV5	Al88-Co10-Ce2	Al78.2-Co15.5-Ce6.3
April PTS A3	Al88-Co10-Ce2	Al84.7-Co11.0-Ce4.3

SEM Images of the Al₈₈Co₁₀Ce₂ at% Feedstock Powder



- The nominal composition is Al₈₈Co₁₀Ce₂ at%.
- Semi-quantitative EDS results indicate the actual coating composition varies spatially and between samples.
- There is generally good agreement between the expected and actual composition.

XRD Spectra



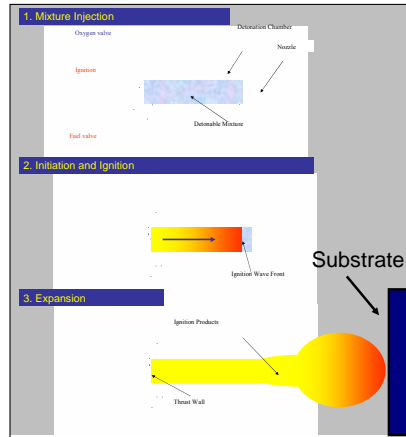
• The composition of the PTS coating and feedstock powder is Al₈₈Co₁₀Ce₂ at%; the composition of the MSR is Al₈₄Co_{7.5}Ce_{8.5} at%.

• The PTS and feedstock powder diffraction peaks correspond with fcc Al.

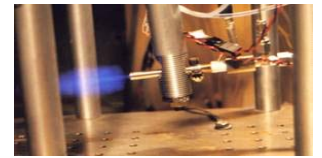
• The PTS coating was heat treated at 275 °C for 6 hours and 285 °C for 3 hours.

KEY RESULT A nanocrystalline PTS coating with possible intermetallic compounds forms after heat treating.

PTS Fabrication Process⁵



PTS Prototype In Action⁵



- The sprayed samples in this study were formed by depositing an Al-Co-Ce alloy onto an AA 2024-T3 or Al-6XN stainless steel substrate using the PTS (Pulsed Thermal Spray) process.
- Cooling rates for < 20 μm particle sizes can reach 106 K/s.⁵
- Coating thickness range from 75 to 600 μm.
- Purging gas, stand off distance, and powder flow rate are just a few of the variables for each coating.

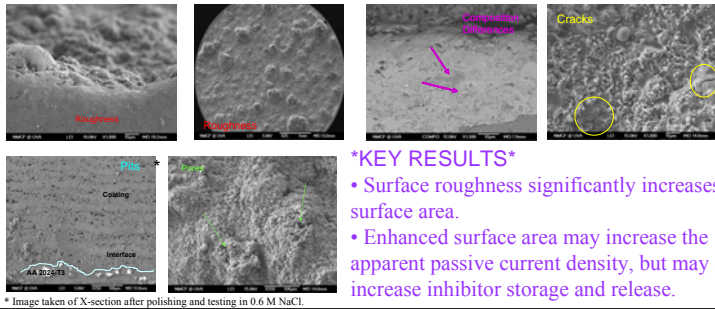
* Tests in table below performed in 0.6 M NaCl, deaerated.

PTS Coating Conditions

Spray Group/Dates	Samples	Composition (at%)	Composition (wt%)	Coating Thickness (micrometers)	Substrate Material	E _{OCP} PTS > E _{PIT} 2024		E _{OCP} PTS < E _{OCP} 2024	
						Epit Range Lo/Hi (V vs SCE)	Epit Range Lo/Hi (V vs SCE)	GCP Range Lo/Hi (V vs SCE)	GCP Range Lo/Hi (V vs SCE)
March 2006	A1-A8, A1A	Al85-Co8-Ce7	Al61-Co16-Ce23	125-250	AA 2024-T351	-0.698 / -0.632	-0.878 / -0.820		
July 2006	A2	Al85-Co8-Ce7	Al61-Co16-Ce23	200	AA 2024-T351	-0.695	-0.889		
06-29-2006	A1, A3-A4	Al85-Co8-Ce7	Al61-Co16-Ce23	200	AA 2024-T351	-0.717 / -0.629	-0.901 / -0.794		
07-07-2006	A6, A8-A12, A14	Al88-Co10-Ce2	Al73-Co18-Ce9	200	AA 2024-T351	-0.658 / -0.592	-0.852 / -0.788		
07-07-2006	A16	Al88-Co10-Ce4	Al67-Co17-Ce16	200	AA 2024-T351	-0.636	-0.797		
December 2006	A1-A2, A5-A12	Al88-Co10-Ce2	Al73-Co18-Ce9	200-400	AA 2024-T351	-0.657 / -0.592	-0.865 / -0.795		
12-12-2006	A6-A8, A11	Al88-Co10-Ce2	Al73-Co18-Ce9	400-500	AA 2024-T351	-0.613 / -0.493	-0.879 / -0.812		
12-13-2006	A2-A4	Al88-Co10-Ce2	Al73-Co18-Ce9	500	AA 2024-T351	-0.626 / -0.502	-0.875 / -0.851		
February 2007	A1-A7, A12	Al88-Co10-Ce2	Al73-Co18-Ce9	150-600	AA 2024-T351	-0.698 / -0.498	-0.823 / -0.707		
02-12-2007	A8-A9	Al88-Co10-Ce2	Al73-Co18-Ce9	600	Removed	-0.651 / -0.636	-0.729 / -0.719		
02-12-2007	A10-A11	Al88-Co10-Ce2	Al73-Co18-Ce9	300-600	AL-6XN	-0.617 / -0.608	-0.740 / -0.671		
April 2007									
04-26-2007	A1-A4	Al88-Co10-Ce2	Al73-Co18-Ce9	400-500	AA 2024-T351	-0.78 / -0.38	-0.78 / -0.76		
May 2007									
05-01-2007	AV1-AV7	Al88-Co10-Ce2	Al73-Co18-Ce9	75-150	AA 2024-T351	-0.781 / -0.29	-0.805 / -0.609		

Surface Features and Real Area

SEM Micrographs of Common PTS Coating Surface Features



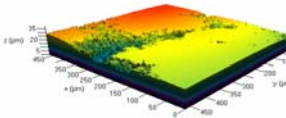
KEY RESULTS

- Surface roughness significantly increases the surface area.
- Enhanced surface area may increase the apparent passive current density, but may also increase inhibitor storage and release.

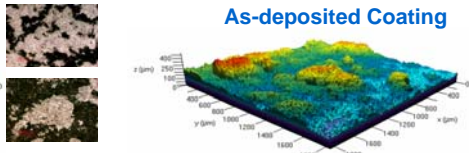
Confocal Micrographs

• The area can be determined directly by the confocal microscope.

Polished Coating



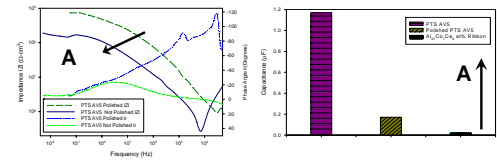
As-deposited Coating



• The surface area can also be measured from impedance/ capacitance data. The area increases with increasing capacitance.

KEY RESULT

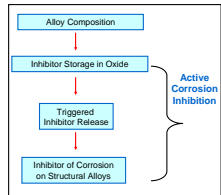
Initial confocal results indicate the surface area of the polished coating is 123% the nominal area, and the as-deposited coating is 397% the nominal area.



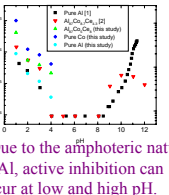
Tests in 0.6 M NaCl, deaerated, after 5 min. OCP hold.

Sacrificial Anodic Behavior and Inhibitor Release Capability

Steps for Active Corrosion Inhibition?

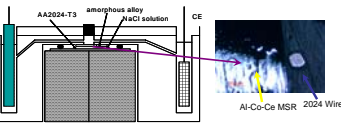


i_{pass} vs. pH for Select Al Alloys⁸



• Due to the amphoteric nature of Al, active inhibition can occur at low and high pH.

Small Volume Cell Schematic



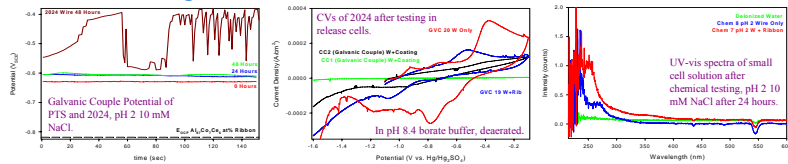
- The cell holds ~20 μ L of solution.
- The AA 2024-T3 wire and Al-Co-Ce alloy can be chemically or galvanically coupled.
- The solution can be analyzed for Ce^{3+} release.

Optical Micrographs of 2024 Wires after Testing



• All cells were exposed to pH 2 10 mM NaCl for 48 Hours.

Advanced Testing of AA 2024-T351 Wires

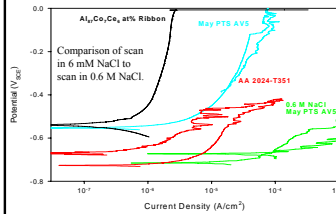


KEY RESULTS

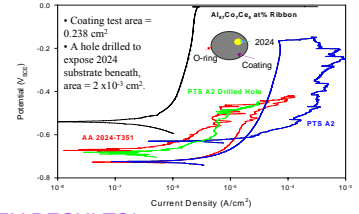
- AA 2024-T351 Wires galvanically coupled to $Al_{10}Co_1Ce_8$ at% MSR or Coating experience pitting corrosion and less overall damage than wire only tests.
- The amount of Cu replated for the AA 2024-T351 wires dramatically decreases when the Wire is coupled to a MSR or PTS coating. The amount of replated Cu in the cyclic voltammogram (CV) is an indicator of the amount of the corrosion damage on the AA 2024-T351 wires.
- The couple potential of the AA 2024-T351 wire and PTS coating increases initially, but tends to stabilize after 24 hours. Therefore sacrificial protection is feasible by the PTS coating.
- Peak analysis of the red curve (UV-vis result) indicates Ce^{3+} was released from the $Al_{10}Co_1Ce_8$ at% MSR present in the cell during the experiment.

Barrier Properties

Effect of [Cl⁻]



Effect of Added Defect

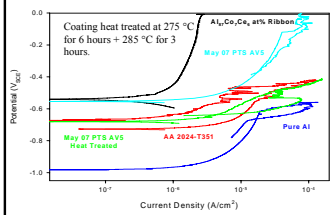


KEY RESULTS

Factors in Barrier Properties:

- The barrier properties of the PTS coatings are approaching those of the MSR, the gold standard.
- Drilling a hole in the coating has proven that defects in the coating are detectable, therefore pores and cracks visible in the coating must not penetrate to the substrate.
- Intermetallics formed upon heat-treatment of the coating are detrimental to the barrier properties of the coating (Al nanocrystals are not).⁶

Effect of Heat Treatment



All samples tested in 6 mM NaCl, neutral pH, deaerated, after a 5 min. OCP hold, 25 °C; test area ~8 x 10⁻³ cm², ~10⁻⁴ cm² for MSR, unless noted.

Conclusions

- The best Al-Co-Ce coating ideally has a combination of good barrier, sacrificial anode, and inhibitor qualities.
- The PTS coating powders have FCC Al crystalline phases present. These phases remain in the deposited coating.
- The heat-treated PTS coating, with intermetallics present, performed worse in electrochemical testing than the as-deposited PTS coating, suggesting that structure affects barrier properties.
- The coatings show potential to be a good barrier with E_{PTT} above AA 2024-T351 and approaching that of Al-Co-Ce MSR.
- Enhanced surface roughness of the spray coatings may allow for more inhibitor release from the coating, thereby providing more protection to AA 2024-T351 wires.
- Small volume release experiments indicate the PTS coating is more effective protecting AA 2024-T351 wire than Al-Co-Ce MSR. The corrosion mode changed to smaller pits in AA 2024-T351 and less Cu was replated during CVs.

Acknowledgements

- This work was supported by a Multi-University Research Initiative (Grant No. F49602-01-0352) and an Air force STTR Phase I and Phase II (Contract No. FA 9550-U6-C-0077) under the direction of Dr. Jennifer Gresham at AFOSR.
- Thanks are given to Shmuel Eidelman at SAIC, Ben Gauthier and David Book at Enigmatics, Inc., the groups at NSWCCD and the Gardner Thermal Spray Company for their participation in the processing efforts, and Dr. Angela Moran at the United States Naval Academy for her assistance.
- Thanks also to Prof. John Scully, my advisor, for his direction and encouragement.
- Appreciation for their contributions and assistance is offered to Prof. Jim Fitz-Gerald, Tomo Aburada, and the other members of CESE at the University of Virginia, as well as Francisco Presuel-Moreno at the Florida Atlantic University.

References

1. A. Inoue, K. Ohtera, K. Kita, and T. Masumoto, Jpn. J. Appl. Phys., Part 2, **27**, L1796 (1998).
2. M.E. Goldman, N.Unlu, G.J. Shiflet, and J.R. Scully, Electrochem. and Solid State Letters, **8** (2) B1-B5 (2005).
3. H.J. Kim, K.M. Lim, B.G. Seong, and C.G. Park, J. Mat. Sci., **36** 49-54 (2001).
4. M.E. Goldman, J.R. Scully, Tunable Barrier Corrosion Properties of Aluminum-Based Metallic Glasses, MS Thesis, University of Virginia, Charlottesville, VA, 2004.
5. Courtesy of D. Book, B. Gauthier of Enigmatics Inc. and S. Eidelman of SAIC.
6. A.M. Lucente, J.R. Scully, Electrochem. Solid-State Lett., **10** (2007).
7. M.A. Jakab, J.R. Scully, Nature Mat., **4** (2005).
8. F.J. Presuel-Moreno, M.E. Goldman, et al., Electrochem., **152**, 8 (2005).